# Longitudinal stability of progression-related microglial activity during teriflunomide treatment in patients with multiple sclerosis

Lehto, Jussi; Nylund, Marjo; Matilainen, Markus; Sucksdorff, Marcus; Vuorimaa, Anna; Rajander, Johan; Wahlroos, Saara; Hariri, Parisa; Airas, Laura

*Published in:*
European Journal of Neurology

*DOI:*
10.1111/ene.15834

Published: 01/08/2023

*Document Version*
Final published version

*Document License*
CC BY

Received: 14 October 2022 | Accepted: 1 May 2023

DOI: 10.1111/ene.15834

european journal of neurology
the official journal of the european academy of neurology

ORIGINAL ARTICLE

# Longitudinal stability of progression-related microglial activity during teriflunomide treatment in patients with multiple sclerosis

Jussi Lehto[1,2] | Marjo Nylund[1,3] | Markus Matilainen[1,3] | Marcus Sucksdorff[1,2,3] | Anna Vuorimaa[1,2,3] | Johan Rajander[1,4] | Saara Wahlroos[1] | Parisa Hariri[1] | Laura Airas[2,3]

[1]Turku PET Centre, Turku, Finland

[2]Neurocenter, Turku University Hospital, Turku, Finland

[3]Clinical Neurosciences, University of Turku, Turku, Finland

[4]Åbo Akademi University, Turku, Finland

**Correspondence**
Jussi Lehto, Neurocenter, Turku University Hospital, Turku, Finland.
Email: juleht@utu.fi

**Funding information**
Academy of Finland; European Committee for Treatment and Research in Multiple Sclerosis; Sanofi Genzyme; Sigrid Juséliuksen Säätiö

## Abstract

**Background and purpose:** The aim was to study brain innate immune cell activation in teriflunomide-treated patients with relapsing–remitting multiple sclerosis.

**Methods:** Imaging with 18-kDa translocator protein positron emission tomography (TSPO-PET) using the [$^{11}$C]PK11195 radioligand was employed to assess microglial activity in the white matter, thalamus and areas surrounding chronic white matter lesions in 12 patients with relapsing–remitting multiple sclerosis who had been treated with teriflunomide for at least 6 months before inclusion. Magnetic resonance imaging (MRI) was used to measure lesion load and brain volume, and quantitative susceptibility mapping (QSM) was used to detect iron rim lesions. These evaluations were repeated after 1 year of inclusion. Twelve age- and gender-matched healthy control subjects were imaged for comparison.

**Results:** Half of the patients had iron rim lesions. In TSPO-PET, the proportion of active voxels indicating innate immune cell activation was slightly greater amongst patients compared with healthy individuals (7.7% vs. 5.4%, $p = 0.033$). The mean distribution volume ratio of [$^{11}$C]PK11195 was not significantly different in the normal-appearing white matter or thalamus amongst patients versus controls. Amongst the treated patients, no significant alteration was observed in positron emission tomography distribution volume ratio, the proportion of active voxels, the number of iron-rim-positive lesions, lesion load or brain volume during follow-up.

**Conclusions:** Compared to controls, treated patients exhibited modest signs of diffuse innate immune cell activity, which was unaltered during follow-up. Lesion-associated smoldering inflammation was negligible at both timepoints. To our knowledge, this is the first study applying both TSPO-PET and QSM-MRI to longitudinally evaluate smoldering inflammation.

KEYWORDS
magnetic resonance imaging, multiple sclerosis, positron emission tomography, quantitative susceptibility mapping, teriflunomide

## INTRODUCTION

Multiple sclerosis (MS) is a leading cause of disability in younger adults in the Western world [1, 2], and microglial activation is a hallmark of progression-related MS pathology. Chronic slowly expanding lesions are characterized by a perilesional ring of activated microglia, whilst inactive plaques contain low numbers of innate immune cells or other inflammatory cells [3, 4]. Quantitative susceptibility mapping (QSM) is an experimental magnetic resonance imaging (MRI) method able to capture susceptibility changes caused by, for example, iron deposition within microglia [5], and iron containing CD68+ microglia and macrophages have been identified around QSM-positive MS lesions with immunohistochemistry [6].

Used in over 500 patients with MS, positron emission tomography (PET) imaging utilizing the 18-kDa translocator protein (TSPO) binding radioligand [$^{11}$C]PK11195 is an established in vivo method to monitor smoldering inflammation in the MS brain [7, 8]. Whilst a subset of astrocytes and endothelial cells may contribute to the TSPO signal, microglia and macrophages constitute the main source of TSPO within the normal-appearing white matter (NAWM) and at the edge of lesions [9–11].

In addition to correlating with disability, as measured with the Expanded Disability Status Scale (EDSS) [12], [$^{11}$C]PK11195 uptake predicts the development of clinically definite MS [13] and disease progression independent of relapse [14]. Interventions with disease-modifying treatments (DMTs) reduce TSPO binding at chronic MS lesions [15, 16] and also in the NAWM [15]. By linking disability progression to microglial activation in the NAWM [17], TSPO-PET has been instrumental in expanding the investigational scope of the pathophysiological process beyond conventional lesions seen with MRI.

Teriflunomide is a treatment for relapsing–remitting MS (RRMS) first introduced almost a decade ago. Of interest is its efficacy in preventing EDSS-measured disability progression in two phase III trials in patients with relatively active MS [18, 19]. As the more recent real-world use of teriflunomide has concentrated on milder MS, this non-interventional study enrolled patients at risk of disease progression based on relatively advanced age, which is one of the strongest known predictors of progression [20]. Patients with secondary progressive MS (SPMS) exhibited increased microglial activation compared with patients with RRMS [21]. Thus, it was of interest to assess TSPO binding in a real-world non-interventional setting of first-line DMT use amongst middle-aged patients at progression risk.

## MATERIALS AND METHODS

### Study design

This was an open-label, non-interventional study performed at the Turku University Hospital Neurocenter and Turku PET Centre, part of the University of Turku, and Turku University Hospital. Although the study was non-interventional regarding teriflunomide treatment, it was interventional regarding TSPO-PET imaging. The study protocol was approved by the Ethics Committee of the Hospital District of Southwest Finland. The study was registered in clinicaltrials.gov (NCT03368677; https://www.clinicaltrials.gov/ct2/show/study/NCT03368677). Study participants provided written informed consent according to the principles of the Declaration of Helsinki, after which they underwent baseline neurological assessments and MRI and TSPO-PET scans within approximately 1 month of inclusion. These baseline assessments and scans were repeated approximately 1 year after the initial PET visit.

### Study subjects

Sixteen eligible subjects treated with teriflunomide in the Hospital District of Southwest Finland were recruited between December 2017 and December 2020. Patients with RRMS, who were treated with teriflunomide for at least 6 months before inclusion, between 40 and 55 years of age, with EDSS score between 1.0 and 6.5 and at least nine T2 lesions at baseline MRI, were considered for the study. Key exclusion criteria included pregnancy, serious liver disease and other significant central nervous system (CNS) pathology besides MS. One subject suffered a panic attack in the PET camera and withdrew her consent after the baseline visit. Another subject discontinued teriflunomide due to poor perceived tolerability and was subsequently excluded between visits. Fourteen subjects remained for the entire study duration. One patient was later diagnosed with SPMS from before enrollment and was excluded from the analysis, and another subject was excluded due to failed radioligand synthesis resulting in inadequate injected activity at follow-up imaging. The temporary loss of follow-up resulted in an extended interval of >2 years between the PET scans for one subject, but these data were included in the analysis as an extended follow-up was not expected to produce significant bias. For comparison, 12 age- and gender-matched healthy individuals were imaged at baseline using TSPO-PET and MRI.

### Magnetic resonance imaging and image processing

All subjects underwent 3-T MRI (Philips Ingenia/Philips Ingenuity, Best, The Netherlands) at baseline and after 1 year of follow-up with the following sequences: T1, T2, fluid-attenuated inversion recovery (FLAIR) and 3D high resolution T1. The PET images were co-registered with the respective T1 images for each subject using statistical parametric mapping (SPM8) (Wellcome Trust Center for Neuroimaging, London, UK). Preliminary lesion masks with variable thresholds were first created using the Lesion Segmentation Toolbox (LST) [22] in SPM, after which these preliminary masks were checked and edited to correspond to T1-hypointense chronic MS lesions according to visual inspection. A chronic lesion was defined as measuring >3 mm$^3$ voxels in at least one dimension with the most hypointense voxels below the intensity of normal gray matter.

The perilesional mask used to quantify tracer uptake surrounding chronic lesions was created by dilating the lesion mask by 3 mm and then subtracting the core image from the 3-mm image.

The LST was used to create FLAIR lesion masks for each patient's baseline MRI, and the resulting masks were manually checked for segmentation errors and edited, if necessary, to also include abnormal white matter FLAIR signals in the perilesional area. The masks were then used on the 1-year follow-up images and edited to account for any visible change in lesion volume. Finally, the T1 and FLAIR masks were combined and subtracted from each patient's segmented white matter masks created with LST's lesion-filling tool similar to that described in Sucksdorff et al. [15] to create NAWM masks. The T1 lesion mask images were also used to fill the corresponding T1 image with the LST lesion-filling tool. The filled T1 was then used to segment thalamic volumes with FreeSurfer (https://surfer.nmr.mgh.harvard.edu/) for PET assessments.

To estimate rater-independent changes in T2 lesion volume, nicMSlesions [23] was first used to segment the lesions from baseline FLAIR images; then the longitudinal pipeline of nicMS was employed using the baseline masks as input. The threshold was set to ≥9 voxels to exclude small unspecific T2 hyperintensities of <3 mm in any dimension. Whole brain volume normalized for head size was estimated with SIENAX [24], and thalamic volumes were segmented with FSL FIRST [25].

## Iron rim detection using QSM

The QSM images were processed using the Morphology Enabled Dipole Inversion toolbox with automatic uniform cerebrospinal fluid zero reference (MEDI+0) [26] from the multi-echo gradient echo sequence data. The reconstructed QSM images were then co-registered with the T1 images using SPM12. Lesions manifesting a positive susceptibility value indicating iron were preselected. If the QSM signal was morphologically consistent with a lesion-associated ring, this lesion was determined as a QSM iron rim lesion by visual inspection by two experienced raters. Additionally, ITK-SNAP (http://www.itksnap.org/pmwiki/pmwiki.php) was used to quantify the signal intensity in the perilesional area and to ascertain the relative hypointensity of the respective core.

## [$^{11}$C]PK11195 radioligand production and PET

To produce the radioisotope $^{11}$C, irradiations were performed with a TR-19 (ACSI, Richmond, Canada) cyclotron by proton bombardment of $^{14}$N utilizing the $^{14}$N(p, α)$^{11}$C nuclear reaction. A target gas mixture of 0.2% oxygen in natural nitrogen produced radioactive $CO_2$. Fifteen minutes of irradiation (19 MeV, 40 μA, 41 bar, 20°C) yielded 60 GBq of $^{11}$[C]$CO_2$.

Detailed synthesis steps to produce the radiochemical compound [$^{11}$C]PK11195 from its precursor have been described elsewhere [27, 28]. Briefly, [$^{11}$C]PK11195 was obtained by trapping [$^{11}$C]$CH_3I$ at room temperature into a reaction vessel containing 1.0 mg of precursor (R)-*N*-desmethyl-PK11195 (1-(2-chlorophenyl)-*N*-(1-methylpropyl)-isoquinoline-3-carboxamide) and 8-quinolinol (1 M, 3 μl) in dimethylsulfoxide (200 μl). The reaction mixture was diluted with the high performance liquid chromatography (HPLC) mobile phase (500 μl) before injection into the HPLC system with a Phenomenex Luna column (C18(2), 10 × 250 mm, 10 μm). Acetonitrile/0.01 M $H_3PO_4$ (65/35, v/v) was used as the HPLC mobile phase with a flow rate of 6 ml/min. The product was further purified by SPE cartridge (SepPak C18 light, Waters) and formulated with ethanol (1 ml), phosphate buffer (0.1 M, 8.5 ml) and propylene glycol (1.5 ml).

Sixty minutes of dynamic list mode PET data were acquired twice for each subject with a high resolution research tomograph (Siemens Medical Solutions, Knoxville, TN, USA). At baseline, the mean ± standard deviation (SD) injected dose of radioactivity was 462 ± 73 MBq for the teriflunomide-treated patients with MS, and 486 ± 17 MBq for the age-matched controls. At 1-year follow-up, the injected dose of radioactivity was 480 ± 52 MBq for teriflunomide-treated patients. No significant dose differences between the groups or timepoints were observed.

## Positron emission tomography data processing and analysis

Image reconstruction was performed with the OP-OSEM algorithm [29] using 17 timeframes. PET image post-processing followed a previously described procedure [15]. Briefly, the dynamic images were smoothed, realigned and co-registered using SPM8. Images were then resliced to match the 1-mm voxel size of the MRI images.

Specific binding of [$^{11}$C]PK11195 was quantified using distribution volume ratios (DVRs). As no reliable anatomical region devoid of activated microglia (i.e., specific PK11195 binding) exists, time–activity curves representing a region without specific binding were acquired with the MATLAB (MathWorks Inc., Natick, MA, USA) software Super-PK using a supervised cluster algorithm [30] optimized with four predefined kinetic tissue classes [31]. The Logan variant reference tissue model [32] with a 20- to 60-min time interval was applied to the regional time–activity curves.

To determine the proportions of individual active voxels, the mean DVR (± SD) of all voxels in the NAWM of healthy control subjects was first calculated. A 95% confidence threshold was determined with the formula mean + 1.96 × SD, which was used for dichotomous classification of each voxel of all subjects, that is, values above the threshold signified an active voxel. Based on our previous data from healthy controls [33], this threshold was set to 1.56. Clusters below the three connected voxels were excluded to prevent the inclusion of random peak values.

Parametric DVR maps of one subject's baseline and follow-up lesion masks dilated 3 mm in each direction were laid on top of T1 MRI images from the respective timepoints using Mango (https://mangoviewer.com/) to produce an illustration of perilesional [$^{11}$C]PK11195 binding. Surface plots from individual lesions were created using Fiji (https://imagej.net/software/fiji/).

### Analysis of chronic lesion subtypes according to microglial activation

Lesion phenotyping was performed according to Nylund et al. [33]. Briefly, individual lesions in the T1 lesion masks were classified into "inactive", "overall active" and "rim active" based on the presence and distribution of active voxels in the core versus rim. Chronic T1 lesions with a minimum volume of 27 $mm^3$ were considered.

### Statistical analysis

The statistical analysis was performed using R version 4.1.1 (https://www.r-project.org/about.html) and SAS version 9.4 (SAS Institute Inc.). The Wilcoxon rank-sum test was used for comparisons between controls and patients, and the Wilcoxon signed-rank test was used to compare the baseline and follow-up measurements of the patients. Gender comparisons were performed using Fisher's exact test. All tests were two-tailed, and $p$ values less than 0.05 were considered as statistically significant for all analyses.

## RESULTS

### Study subjects

The teriflunomide-treated cohort ($n = 12$) consisted of three males and nine females of Caucasian descent with an average (± SD) age and disease duration of 46.1 ± 6.2 and 10.8 ± 8.1 years, respectively. The mean (± SD) duration of teriflunomide treatment was 10 ± 3.5 months before baseline imaging. The demographic baseline characteristics are listed in Table 1.

**TABLE 1** Demographics and lesion phenotyping

| ID (M/F) | Timepoint | Disease duration | EDSS | ARR before inclusion | Rim active | Overall active | Inactive | QSM+ |
|---|---|---|---|---|---|---|---|---|
| P01 (F) | Baseline | 12.12 | 1.5 | 0.25 | 0 | 0 | 2 | 0 |
| | Follow-up | | 2.5 | | 0 | 2 | 0 | 0 |
| P02 (F) | Baseline | 6.43 | 3.5 | 0.16 | 1 | 2 | 8 | 0 |
| | Follow-up | | 3.0 | | 0 | 3 | 8 | 0 |
| P03 (F) | Baseline | 3.56 | 1.5 | 0.28 | 0 | 4 | 1 | 2 |
| | Follow-up | | 2.0 | | 2 | 1 | 2 | 2 |
| P04 (F) | Baseline | 7.29 | 2.5 | 0.14 | 1 | 3 | 1 | 2 |
| | Follow-up | | 4.0 | | 1 | 2 | 3 | 2 |
| P05 (F) | Baseline | 12.56 | 2.0 | 0.32 | 1 | 4 | 2 | 1 |
| | Follow-up | | 2.0 | | 1 | 4 | 2 | 1 |
| P06 (F) | Baseline | 21.64 | 2.5 | 0.32 | 1 | 2 | 5 | 1 |
| | Follow-up | | 2.5 | | 1 | 2 | 5 | 1 |
| P07 (F) | Baseline | 7.89 | 2.0 | 0.25 | 0 | 2 | 2 | 2 |
| | Follow-up | | 2.0 | | 1 | 4 | 0 | 2 |
| P08 (F) | Baseline | 29.83 | 3.5 | 0.70 | 0 | 0 | 2 | 0 |
| | Follow-up | | 3.5 | | 0 | 1 | 1 | 0 |
| P09 (F) | Baseline | 14.43 | 3.0 | 0.14 | 0 | 2 | 1 | 0 |
| | Follow-up | | 2.0 | | 0 | 2 | 1 | 0 |
| P10 (M) | Baseline | 9.64 | 1.0 | 0.21 | 0 | 1 | 3 | 0 |
| | Follow-up | | 1.0 | | 0 | 1 | 3 | 0 |
| P11 (M) | Baseline | 3.21 | 1.5 | 0.62 | 0 | 1 | 1 | 0 |
| | Follow-up | | 2.0 | | 0 | 0 | 1 | 0 |
| P12 (M) | Baseline | 0.76 | 2.0 | 1.32 | 2 | 6 | 7 | 5 |
| | Follow-up | | 2.5 | | 2 | 7 | 6 | 5 |
| Mean ± SD or median (IQR) | Baseline | 11.0 ± 8.1 | 2 (1.5–2.62) | 0.25 (0.18–0.32) | | | | |
| | Follow-up | N/A | 2.25 (2–2.75) | N/A | | | | |

Abbreviations: +, positive; ARR, annualized relapse rate; EDSS, Expanded Disability Status Scale; F, female; IQR, interquartile range; M, male; QSM, quantitative susceptibility mapping; SD, standard deviation.

**TABLE 2** MRI variables

| MRI variables | Baseline | 1-year follow-up | *p* value |
|---|---|---|---|
| Brain volume, $cm^3$ | | | |
| MS | 1516 (1489–1556) | 1521 (1482–1540) | 0.2 |
| HC | 1569 (1546–1611) | | |
| *p* value (MS vs. HC) | 0.010† | | |
| Thalamus volume, $cm^3$ | | | |
| MS | 14.4 (13.7–15.2) | 14.3 (13.9–15.0) | 0.13 |
| HC | 16.1 (15.5–16.8) | | |
| *p* value (MS vs. HC) | 0.010† | | |
| T2 lesion volume, $cm^3$ | 2.29 (1.18–3.27) | 2.33 (1.67–3.25) | 0.092 |

*Note*: Values are median (IQR).

Abbreviations: HC, healthy control; IQR, interquartile range; MRI, magnetic resonance imaging; MS, patient with multiple sclerosis.

†Statistically significant.

## Clinical and conventional MRI parameters at baseline and follow-up amongst patients with MS

The median and interquartile range (IQR) EDSS score was 2 (1.5–2.62) at baseline and 2.25 (2–2.75) at follow-up. There were no serious adverse events, and no subjects suffered documented MS relapses. Focal T2 lesion burden was modest with a median (IQR) of 2.3 (1.2–3.3) $cm^3$ T2 lesion volume per patient, and no significant alteration was observed in the lesion volume during follow-up (Table 2). At the individual lesion level, the median (IQR) volumes were 32 (17–101) $mm^3$ and 34 (18–100) $mm^3$ at baseline and follow-up, respectively, and no significant change in the number of T2 lesions of >8 voxels was detected with a median (IQR) of 19.5 (13.5–24.5) and 18.5 (14.0–25.5) at baseline and follow-up, respectively ($p > 0.05$). Whole brain and thalamic volumes were somewhat smaller amongst patients compared with controls, with no significant change during follow-up in either (Table 2).

## Translocator protein PET binding amongst patients versus controls

Comparing TSPO binding between patients with MS and healthy controls, no baseline difference in TSPO availability (measured as DVR) was observed in any examined region (whole brain, NAWM, and thalamus) (Figure 1a–c). The mean (± SD) baseline DVRs of [$^{11}$C]PK11195 were 1.17 ± 0.03 and 1.17 ± 0.03 ($p = 0.84$) in the NAWM and 1.31 ± 0.05 and 1.28 ± 0.06 ($p = 0.27$) in the thalamus for patients versus controls, respectively. The presence of active voxels, that is, voxels with DVR > 1.56, was then evaluated and it was found that patients with MS had a greater baseline proportion of active voxels compared with controls (7.7% ± 2.9% vs. 5.4% ± 1.7%, $p = 0.033$), indicating modest innate immune cell activation (Figure 1d–f). When studied separately in the thalamus and NAWM, trends in the proportions of active voxels were similar but not statistically different (thalamus, 21.1% ± 5.5% vs. 16.0% ± 7.3%, $p = 0.14$; NAWM, 7.0% ± 2.5% vs. 5.2% ± 2.0%, $p = 0.052$, respectively).

## Longitudinal stability of TSPO availability during teriflunomide treatment

The low level of baseline microglial activation remained stable during follow-up: whilst there was a slight trend downwards, there were no statistically significant DVR changes in the NAWM, thalamus or perilesional area between baseline and follow-up (Figure 2a–d). In the perilesional area, the baseline and follow-up DVRs were 1.15 ± 0.08 and 1.11 ± 0.08 ($p = 0.13$). In line with the DVR PET results, the proportion of active voxels remained stable during teriflunomide treatment in all examined brain areas (Figure 2e–h).

## Prevalence of chronic active lesions at baseline based on TSPO-PET and QSM-MRI

Thirteen chronic lesions with iron rims were observed amongst six of 12 patients with MS at baseline and this number remained stable at follow-up. Similarly, according to our previously described TSPO-PET-based classification [33], six patients with MS had chronic rim active lesions at follow-up. Although the QSM-positive lesions did not reliably co-localize with PET-based rim activity, all patients with QSM-positive lesions had rim active lesions at follow-up, whilst none of the QSM-negative patients had rim active lesions at follow-up (Table 1). There were 35 chronic inactive lesions at baseline, with all patients having chronic inactive lesions. The number of overall active lesions was 27, with an average of 2.2 lesions per patient. All patients had overall active lesions either at baseline or at follow-up (Table 1). The majority (eight of 13) of QSM+ lesions were classified as overall active in PET at baseline.

# DISCUSSION

Translocator protein availability remained largely unaltered during the 1-year follow-up in this cohort of teriflunomide-treated patients

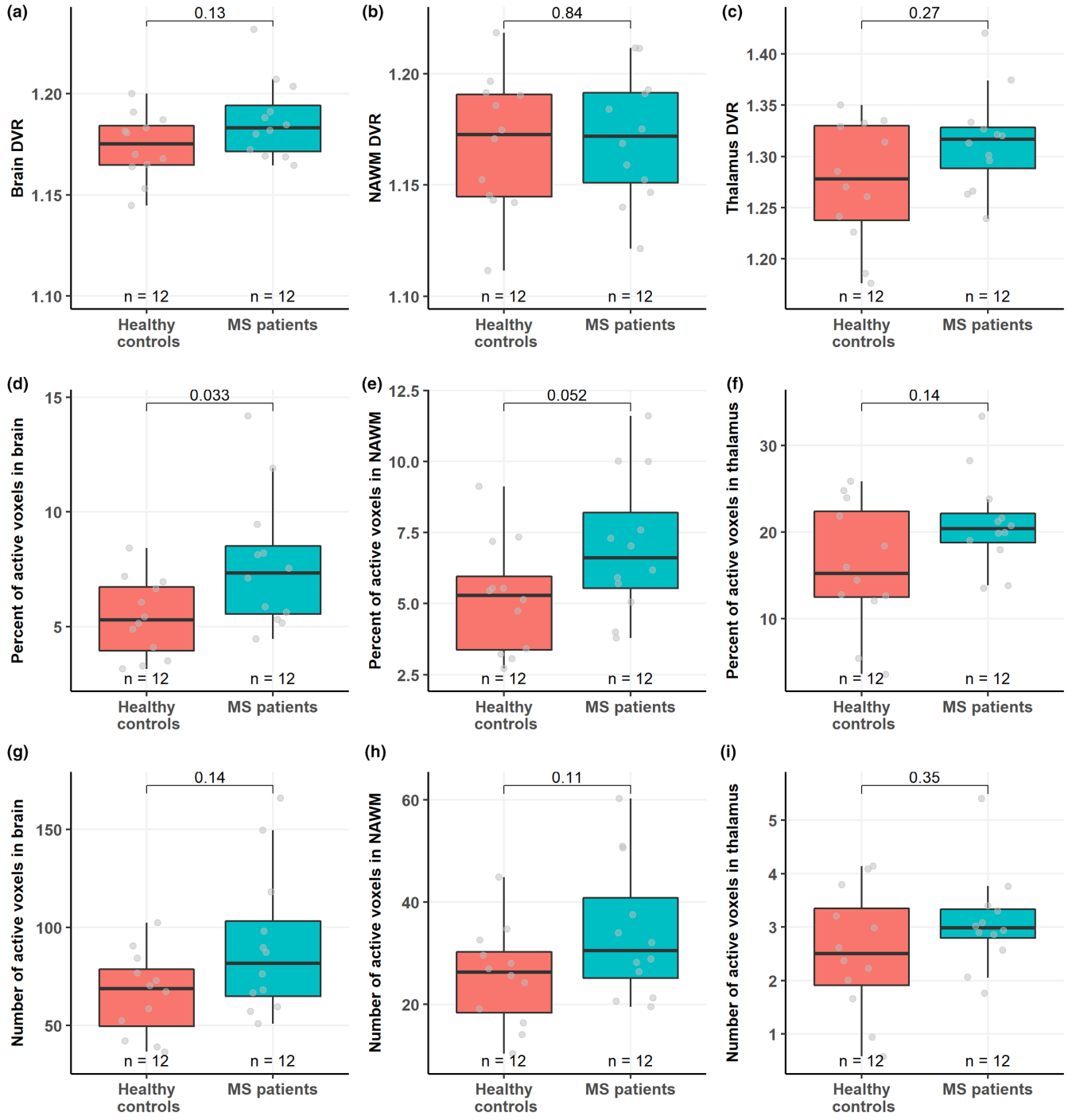


**FIGURE 1** [$^{11}$C]PK11195 distribution volume ratio (DVR) comparisons in the whole brain (a), normal-appearing white matter (NAWM) (b) and thalamus (c) demonstrated no difference in 18-kDa translocator protein (TSPO) availability between patients with multiple sclerosis (MS) and healthy controls at baseline. The proportions (d)–(f) and absolute numbers (g)–(i) of active voxels were consistent with the DVR results.

with RRMS. Furthermore, only a modest difference in brain microglial activation was observed between the RRMS population and an age-matched healthy control population. However, this difference manifested as a statistically significant difference in the proportion of active voxels in the MS versus control brain. No difference in the DVR values in the whole brain, NAWM or thalamus regions of interest was observed between patients and controls. This finding implies that TSPO-PET-based detection of clusters of active voxels in the MS brain may be a more sensitive method for capturing innate immune cell activation compared with quantifying radioligand binding using DVR in various brain regions of interest.

In other MS cohorts, significantly higher DVR values in MS brain NAWM compared to control white matter [13, 15, 16] have been previously repeatedly demonstrated by ourselves and others. It has

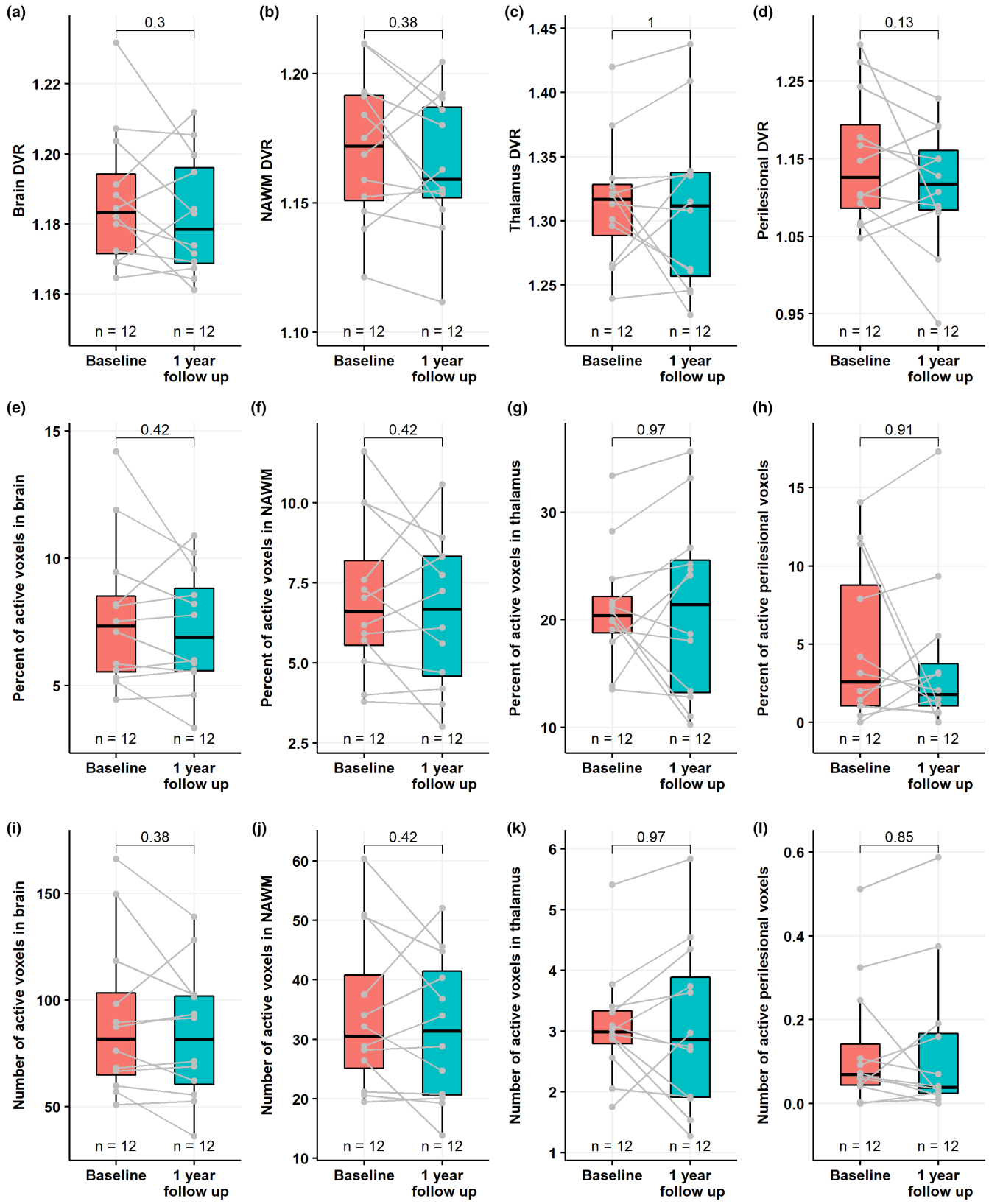


**FIGURE 2** [$^{11}$C]PK11195 distribution volume ratio (DVR) comparisons in the whole brain (a), normal-appearing white matter (NAWM) (b), thalamus (c) and the perilesional area (d) demonstrated no alteration in 18-kDa translocator protein (TSPO) availability during 1-year treatment with teriflunomide in these regions of interest. Similarly, no significant differences were seen in the proportions (e)–(h) or absolute numbers (i)–(l) of active voxels.

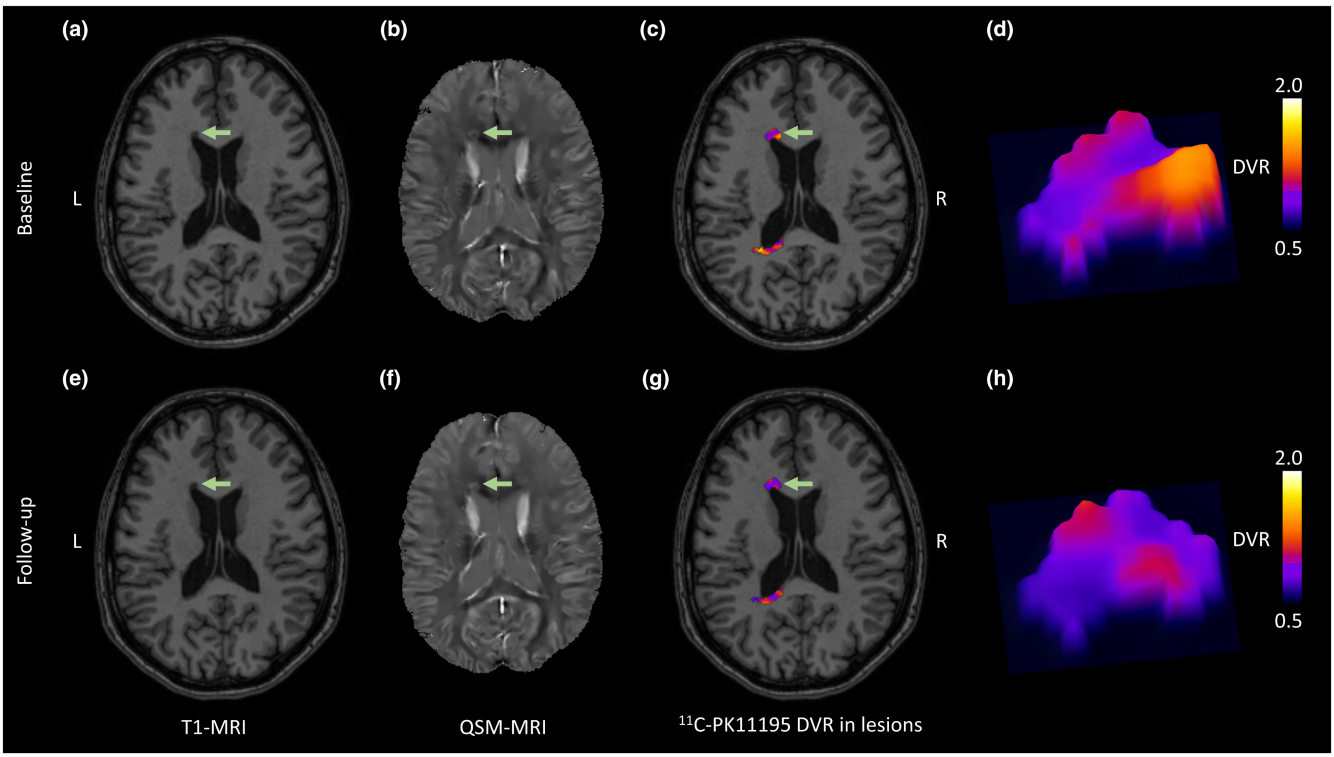


**FIGURE 3** An example of an overall active lesion (P03) in T1 (a), quantitative susceptibility mapping (QSM) (b) and positron emission tomography (PET) overlaid on T1 (c) at baseline (a)–(c) and 1-year follow-up (e)–(g). The 3d surface plots (d), (h) represent PET distribution volume ratio (DVR) at baseline and follow-up, respectively, and the arrows point to the examined lesion. Whilst this lesion is not rim active according to our classification, a higher QSM intensity appears to co-localize with higher PET DVR at the lesion edge. L, left; R, right.

been demonstrated previously that higher TSPO-DVR both in the NAWM and thalamus [14, 34] predicts a greater likelihood of later disease progression, which is an indicator of the detrimental nature of TSPO-PET-measurable innate immune cell activation. Moreover, this finding may have implications for patient recruitment for future clinical trials targeting innate immune cell activation and slowing down disease progression or for clinical treatment stratification.

During the last decade, MS treatment has shifted towards early escalation and early intense treatment approaches [35]. This shift has happened at the expense of recent phase III trials [36, 37], where relatively less active cohorts of patients were enrolled compared with past trials [18, 19]. Although the more recent trials successfully demonstrated relative efficacy with limited effect size in RRMS in terms of the annualized relapse rate, prerequisites for successful trials on patients with SPMS should include concentrated efforts to better characterize the population at a high risk of progression.

Although conversion to secondary progression occurs on average at 45 years of age [38], MS is a heterogeneous disease, and, despite the relatively advanced age (46 years) and long disease duration (11 years) of the RRMS cohort included in the present study, only modest signs of TSPO-PET-measurable innate immune cell activation were visible, indicating a lower risk for disease progression in the near future. Additionally, the relatively high proportion of inactive lesions (>50% at baseline) and the low number of rim active lesions (six at baseline) suggest a lower risk of progression. A larger RRMS cohort ($n = 67$) of comparable EDSS (median 2.5), with a dissimilar distribution of inactive (34%) and rim active (16%) lesions, has been previously characterized, and it has been shown that rim active lesion load correlates with disability [33].

It is difficult to estimate exactly what impact teriflunomide treatment had on the longitudinally stable TSPO-PET findings in this cohort. It has been previously demonstrated in an untreated MS cohort with more accrued disability (EDSS = 6) that TSPO binding increased over 1-year follow-up both in the NAWM and perilesional areas [15].

Teriflunomide limits the activation and proliferation of lymphocytes by inhibiting pyrimidine biosynthesis in activated lymphocytes via the mitochondrial enzyme dihydroorotate dehydrogenase [39]. Further to these peripheral effects, effects on resident CNS cells (oligodendrocytes and microglia) have been suggested based on in vitro and experimental animal work [40–42]. In rodents, teriflunomide crosses the blood–brain barrier with 1%–2% of serum concentrations (in the range 2.5–4.1 μM) reaching the CNS [43]. Thus, in theory, teriflunomide may have contributed to the unaltered microglial status via either peripheral or central effects.

From a health economic perspective, the correct timing of de-escalation or complete cessation of treatment is another unresolved question. Whilst a prior stable disease course does not appear to protect patients from disability after DMT discontinuation [44], discontinuation after a period of inactivity according to conventional clinical parameters was not associated with time to clinical relapse, MRI activity or EDSS increase [45]. The timing of discontinuation is not feasible with PET but based on the presented results and

previous evidence PET may be used to better characterize patients at a low risk of progression.

Other potential and more readily available prognostic biomarkers in MS include cortical MRI lesions [46], QSM [6], thalamic volume [47] and neurofilament light chain [48]. Future next steps include cross-sectional comparisons of these biomarkers with PET. Regarding our study cohort, follow-up including conventional MRI, diffusion tensor imaging, QSM and blood neurofilament light chain is ongoing up to 3 years after inclusion. In this study, only 13 QSM lesions were found, and the relatively short follow-up precluded meaningful correlations with clinical variables. However, QSM positivity seemed to correlate with microglial activity according to visual inspection of parametric PET data (Figures 3 and S1: between-group PET DVRs). Larger longitudinal studies that combine PET and QSM and also enroll patients with more active disease will demonstrate whether QSM is a more readily available surrogate for chronic smoldering inflammation and a possible temporal relationship between QSM intensity and later PET-measurable smoldering rim activity.

Our initial aspiration was to include a cohort that, based on patient age, was at risk of progression. However, as the study was performed in a real-life setting and age is a strong predictor of progression [20], the final study cohort was affected by relatively benign disease based on T2 lesion load (average 2.3 ml), low TSPO-PET DVR (not different from age-matched controls) and a low EDSS (median 2). Commonly employed SPMS criteria [49] require an EDSS of 4. Future trials targeting a population at progression risk would probably benefit from a higher EDSS requirement, although this would complicate recruitment efforts in the current treatment landscape, where active patients are often quickly identified and escalated, if necessary. Ultimately, even if combined, EDSS and age are unlikely to produce the required specificity or sensitivity.

Based on current knowledge, microglial activation contributes to MS progression and, beyond teriflunomide, novel compounds like Bruton's tyrosine kinase inhibitors currently in clinical development for MS may have greater potential to slow progression by suppressing activated microglia. The results of this study are in line with previous indirect evidence of teriflunomide's neuroprotective properties independent of relapse or conventional MRI activity [50]. Furthermore, a direct effect on brain microglia as a contributing mechanism of action cannot be excluded [40].

## AUTHOR CONTRIBUTIONS

**Marjo Nylund:** Conceptualization; project administration; funding acquisition. **Markus Matilainen:** Formal analysis; visualization. **Marcus Sucksdorff:** Investigation; conceptualization. **Anna Vuorimaa:** Investigation. **Johan Rajander:** Resources. **Saara Wahlroos:** Resources. **Parisa Hariri:** Investigation; formal analysis.

## ACKNOWLEDGEMENTS

The authors thank Mikko Koivumäki and Taruliina Parkkali for their valuable support in the execution of this study.

## FUNDING INFORMATION

This work was supported by Sanofi-Genzyme, Finnish Academy (decision number 330902), the Sigrid Juselius Foundation, the state research funding of the Turku University Hospital expert responsibility area, and the InFLAMES Flagship Programme of the Academy of Finland (decision number 337530). P. Hariri's work was funded by ECTRIMS Multiple Sclerosis Postdoctoral Research Fellowship Exchange Programme.

## CONFLICT OF INTEREST STATEMENT

Dr Airas has obtained institutional research support from Novartis, Sanofi-Genzyme and Merck and compensation for lectures and advising from Novartis, Sanofi-Genzyme, Merck, Roche and Janssen. The other authors have nothing to disclose.

## DATA AVAILABILITY STATEMENT

Any anonymized data used in the preparation of this article will be made available on the request of a qualified investigator.

## ORCID

*Jussi Lehto* https://orcid.org/0000-0002-2589-2549

## REFERENCES

1. Kingwell E, Marriott JJ, Jetté N, et al. Incidence and prevalence of multiple sclerosis in Europe: a systematic review. *BMC Neurol*. 2013;13(1):128. doi:10.1186/1471-2377-13-128
2. Pirttisalo AL, Soilu-Hänninen M, Sipilä JOT. Multiple sclerosis epidemiology in Finland: regional differences and high incidence. *Acta Neurol Scand*. 2019;139(4):353-359. doi:10.1111/ane.13057
3. Guerrero BL, Sicotte NL. Microglia in multiple sclerosis: friend or foe? *Front Immunol*. 2020;11:374. doi:10.3389/fimmu.2020.00374
4. Lassmann H. Review: the architecture of inflammatory demyelinating lesions: implications for studies on pathogenesis. *Neuropathol Appl Neurobiol*. 2011;37(7):698-710. doi:10.1111/j.1365-2990.2011.01189.x
5. Wang Y, Liu T. Quantitative susceptibility mapping (QSM): decoding MRI data for a tissue magnetic biomarker. *Magn Reson Med*. 2015;73(1):82-101. doi:10.1002/MRM.25358
6. Kaunzner UW, Kang Y, Zhang S, et al. Quantitative susceptibility mapping identifies inflammation in a subset of chronic multiple sclerosis lesions. *Brain*. 2019;142(1):133-145. doi:10.1093/brain/awy296
7. Chauveau F, Becker G, Boutin H. Have (R)-[$^{11}$C]PK11195 challengers fulfilled the promise? A scoping review of clinical TSPO PET studies. *Eur J Nucl Med Mol Imaging*. 2021;49(1):201-220. doi:10.1007/s00259-021-05425-w
8. Giovannoni G, Popescu V, Wuerfel J, et al. Smouldering multiple sclerosis: the 'real MS'. *Ther Adv Neurol Disord*. 2022;15:1-18. doi:10.1177/17562864211066751
9. Beaino W, Janssen B, Kooij G, et al. Purinergic receptors P2Y12R and P2X7R: potential targets for PET imaging of microglia phenotypes in multiple sclerosis. *J Neuroinflammation*. 2017;14(1):1-16. doi:10.1186/S12974-017-1034-Z/FIGURES/8
10. Nutma E, Stephenson JA, Gorter RP, et al. A quantitative neuropathological assessment of translocator protein expression in multiple sclerosis. *Brain*. 2019;142(11):3440-3455. doi:10.1093/BRAIN/AWZ287
11. Banati RB, Newcombe J, Gunn RN, et al. The peripheral benzodiazepine binding site in the brain in multiple sclerosis: quantitative

in vivo imaging of microglia as a measure of disease activity. *Brain*. 2000;123(11):2321-2337. doi:10.1093/brain/123.11.2321
12. Politis M, Giannetti P, Su P, et al. Increased PK11195 PET binding in the cortex of patients with MS correlates with disability. *Neurology*. 2012;79(6):523-530. doi:10.1212/WNL.0b013e3182635645
13. Giannetti P, Politis M, Su P, et al. Increased PK11195-PET binding in normal-appearing white matter in clinically isolated syndrome. *Brain*. 2015;138:110-119. doi:10.1093/brain/awu331
14. Sucksdorff M, Matilainen M, Tuisku J, et al. Brain TSPO-PET predicts later disease progression independent of relapses in multiple sclerosis. *Brain*. 2020;143(11):3318-3330. doi:10.1093/brain/awaa275
15. Sucksdorff M, Tuisku J, Matilainen M, et al. Natalizumab treatment reduces microglial activation in the white matter of the MS brain. *Neurol Neuroimmunol Neuroinflamm*. 2019;6(4):e574. doi:10.1212/NXI.0000000000000574
16. Sucksdorff M, Rissanen E, Tuisku J, et al. Evaluation of the effect of fingolimod treatment on microglial activation using serial PET imaging in multiple sclerosis. *J Nucl Med*. 2017;58(10):1646-1651. doi:10.2967/jnumed.116.183020
17. Rissanen E, Tuisku J, Rokka J, et al. In vivo detection of diffuse inflammation in secondary progressive multiple sclerosis using PET imaging and the radioligand $^{11}$C-PK11195. *J Nucl Med*. 2014;55(6):939-944. doi:10.2967/jnumed.113.131698
18. Confavreux C, O'Connor P, Comi G, et al. Oral teriflunomide for patients with relapsing multiple sclerosis (TOWER): a randomised, double-blind, placebo-controlled, phase 3 trial. *Lancet Neurol*. 2014;13(3):247-256. doi:10.1016/S1474-4422(13)70308-9
19. O'Connor P, Wolinsky JS, Confavreux C, et al. Randomized trial of oral teriflunomide for relapsing multiple sclerosis. *N Engl J Med*. 2011;365(14):1293-1303. doi:10.1056/NEJMoa1014656
20. Scalfari A, Neuhaus A, Daumer M, Ebers GC, Muraro PA. Age and disability accumulation in multiple sclerosis. *Neurology*. 2011;77(13):1246-1252. doi:10.1212/WNL.0b013e318230a17d
21. Rissanen E, Tuisku J, Vahlberg T, et al. Microglial activation, white matter tract damage, and disability in MS. *Neurol Neuroimmunol Neuroinflamm*. 2018;5(3):e443. doi:10.1212/nxi.0000000000000443
22. Schmidt P, Gaser C, Arsic M, et al. An automated tool for detection of FLAIR-hyperintense white-matter lesions in multiple sclerosis. *Neuroimage*. 2012;59(4):3774-3783. doi:10.1016/j.neuroimage.2011.11.032
23. Weeda MM, Brouwer I, de Vos ML, et al. Comparing lesion segmentation methods in multiple sclerosis: input from one manually delineated subject is sufficient for accurate lesion segmentation. *Neuroimage Clin*. 2019;24:102074. doi:10.1016/j.nicl.2019.102074
24. Smith SM, Zhang Y, Jenkinson M, et al. Accurate, robust, and automated longitudinal and cross-sectional brain change analysis. *Neuroimage*. 2002;17(1):479-489. doi:10.1006/nimg.2002.1040
25. Patenaude B, Smith SM, Kennedy DN, Jenkinson M. A Bayesian model of shape and appearance for subcortical brain segmentation. *Neuroimage*. 2011;56(3):907-922. doi:10.1016/j.neuroimage.2011.02.046
26. Liu Z, Spincemaille P, Yao Y, Zhang Y, Wang Y. MEDI+0: morphology enabled dipole inversion with automatic uniform cerebrospinal fluid zero reference for quantitative susceptibility mapping. *Magn Reson Med*. 2018;79(5):2795-2803. doi:10.1002/mrm.26946
27. Camsonne R, Crouzel C, Comar D, et al. Synthesis of *N*-($^{11}$C) methyl, *N*-(methyl-1 propyl), (chloro-2 phenyl)-1 isoquinoleine carboxamide-3 (PK 11195): a new ligand for peripheral benzodiazepine receptors. *J Labelled Comp Radiopharm*. 1984;21(10):985-991. doi:10.1002/jlcr.2580211012
28. Debruyne JC, Versijpt J, Van Laere KJ, et al. PET visualization of microglia in multiple sclerosis patients using [$^{11}$C]PK11195. *Eur J Neurol*. 2003;10(3):257-264. doi:10.1046/j.1468-1331.2003.00571.x
29. Hong IK, Chung ST, Kim HK, Kim YB, Son YD, Cho ZH. Ultra fast symmetry and SIMD-based projection-backprojection (SSP) algorithm for 3-D PET image reconstruction. *IEEE Trans Med Imaging*. 2007;26(6):789-803. doi:10.1109/TMI.2007.892644
30. Turkheimer FE, Edison P, Pavese N, et al. Reference and target region modeling of [$^{11}$C]-PK11195 brain studies. *J Nucl Med*. 2007;48(1):158-167.
31. Yaqub M, Van Berckel BNM, Schuitemaker A, et al. Optimization of supervised cluster analysis for extracting reference tissue input curves in (R)-[ $^{11}$C]PK11195 brain PET studies. *J Cereb Blood Flow Metab*. 2012;32(8):1600-1608. doi:10.1038/jcbfm.2012.59
32. Logan J, Fowler JS, Volkow ND, Wang GJ, Ding YS, Alexoff DL. Distribution volume ratios without blood sampling from graphical analysis of PET data. *J Cereb Blood Flow Metab*. 1996;16(5):834-840. doi:10.1097/00004647-199609000-00008
33. Nylund M, Sucksdorff M, Matilainen M, Polvinen E, Tuisku J, Airas L. Phenotyping of multiple sclerosis lesions according to innate immune cell activation using 18 kDa translocator protein-PET. *Brain Commun*. 2022;4(1):fcab301. doi:10.1093/braincomms/fcab301
34. Misin O, Matilainen M, Nylund M, et al. Innate immune cell-related pathology in the thalamus signals a risk for disability progression in multiple sclerosis. *Neurol Neuroimmunol Neuroinflamm*. 2022;9(4):e1182. doi:10.1212/NXI.0000000000001182
35. Casanova B, Quintanilla-Bordás C, Gascón F. Escalation vs. early intense therapy in multiple sclerosis. *J Pers Med*. 2022;12(1):1-14. doi:10.3390/jpm12010119
36. Kappos L, Fox RJ, Burcklen M, et al. Ponesimod compared with teriflunomide in patients with relapsing multiple sclerosis in the active-comparator phase 3 OPTIMUM study: a randomized clinical trial. *JAMA Neurol*. 2021;78(5):558-567. doi:10.1001/jamaneurol.2021.0405
37. Hauser SL, Bar-Or A, Cohen JA, et al. ofatumumab versus teriflunomide in multiple sclerosis. *N Engl J Med*. 2020;383(6):546-557. doi:10.1056/nejmoa1917246
38. Tutuncu M, Tang J, Zeid NA, et al. Onset of progressive phase is an age-dependent clinical milestone in multiple sclerosis. *Mult Scler J*. 2013;19(2):188-198. doi:10.1177/1352458512451510
39. Bruneau JM, Yea CM, Spinella-Jaegle S, et al. Purification of human dihydro-orotate dehydrogenase and its inhibition by A77 1726, the active metabolite of leflunomide. *Biochem J*. 1998;336(2):299-303. doi:10.1042/bj3360299
40. Wostradowski T, Prajeeth CK, Gudi V, et al. In vitro evaluation of physiologically relevant concentrations of teriflunomide on activation and proliferation of primary rodent microglia. *J Neuroinflammation*. 2016;13(1):250. doi:10.1186/s12974-016-0715-3
41. Ambrosius B, Faissner S, Guse K, et al. Teriflunomide and monomethylfumarate target HIV-induced neuroinflammation and neurotoxicity. *J Neuroinflammation*. 2017;14(1):51. doi:10.1186/s12974-017-0829-2
42. Prabhakara KS, Kota DJ, Jones GH, Srivastava AK, Cox CS, Olson SD. Teriflunomide modulates vascular permeability and microglial activation after experimental traumatic brain injury. *Mol Ther*. 2018;26(9):2152-2162. doi:10.1016/J.YMTHE.2018.06.022
43. Kaplan J, Cavalier S, Turpault S. Biodistribution of teriflunomide in naïve rats vs rats with experimental autoimmune encephalomyelitis. In: European Committee for Treatment and Research in Multiple Sclerosis, 7–10 October 2015, ECTRIMS, Barcelona; 2015, p. 354.
44. Jakimovski D, Kavak KS, Vaughn CB, et al. Discontinuation of disease modifying therapies is associated with disability progression regardless of prior stable disease and age. *Mult Scler Relat Disord*. 2022;57:103406. doi:10.1016/j.msard.2021.103406
45. Yano H, Gonzalez C, Healy BC, Glanz BI, Weiner HL, Chitnis T. Discontinuation of disease-modifying therapy for patients with relapsing–remitting multiple sclerosis: effect on clinical and MRI outcomes. *Mult Scler Relat Disord*. 2019;35:119-127. doi:10.1016/j.msard.2019.07.021

46. Scalfari A, Romualdi C, Nicholas RS, et al. The cortical damage, early relapses, and onset of the progressive phase in multiple sclerosis. *Neurology*. 2018;90(24):e2107-e2118. doi:10.1212/WNL.0000000000005685
47. Hänninen K, Viitala M, Paavilainen T, et al. Thalamic atrophy predicts 5-year disability progression in multiple sclerosis. *Front Neurol*. 2020;11:606. doi:10.3389/fneur.2020.00606
48. Khalil M. Are neurofilaments valuable biomarkers for long-term disease prognostication in MS? *Mult Scler J*. 2018;24(10):1270-1271. doi:10.1177/1352458518791518
49. Lorscheider J, Buzzard K, Jokubaitis V, et al. Defining secondary progressive multiple sclerosis. *Brain*. 2016;139(9):2395-2405. doi:10.1093/brain/aww173
50. Sprenger T, Kappos L, Radue EW, et al. Association of brain volume loss and long-term disability outcomes in patients with multiple sclerosis treated with teriflunomide. *Mult Scler J*. 2020;26(10):1207-1216. doi:10.1177/1352458519855722

## SUPPORTING INFORMATION

Additional supporting information can be found online in the Supporting Information section at the end of this article.

**How to cite this article:** Lehto J, Nylund M, Matilainen M, et al. Longitudinal stability of progression-related microglial activity during teriflunomide treatment in patients with multiple sclerosis. *Eur J Neurol*. 2023;30:2365-2375. doi:10.1111/ene.15834